Published December 14, 2012

Effects of Mulch Cover Rate on Interrill Erosion Processes and the Size Selectivity of Eroded Sediment on Steep Slopes

Z.H. Shi *
State Key Lab. of Soil Erosion and Dryland Farming on the Loess Plateau
Institute of Soil and Water Conservation
Chinese Academy of Sciences
Yangling, Shaanxi 712100
China

and
College of Resources and Environment
Huazhong Agricultural Univ.
Wuhan 430070
China

B.J. Yue
L. Wang
N.F. Fang
D. Wang
State Key Lab. of Soil Erosion and Dryland Farming on the Loess Plateau
Institute of Soil and Water Conservation
Chinese Academy of Sciences
Yangling, Shaanxi 712100
China

F.Z. Wu
College of Resources and Environment
Huazhong Agricultural Univ.
Wuhan 430070
China

Mulching with vegetative residue is an effective soil conservation practice. A better understanding of sediment characteristics associated with various mulch rates would improve the use of this practice for soil conservation. An experiment was conducted to evaluate the effects of straw mulch on runoff, erosion, and the particle-size distribution (PSD) of eroded sediment. Straw mulch rates of 0, 15, 30, 50, 70, and 90% cover were tested using simulated rainfall. The effective PSD of sediment (undispersed) was compared with equivalent measurements of the same samples after dispersion (ultimate PSD) to investigate the detachment and transport mechanisms involved in sediment mobilization. The maximum stream occurred at a different time from the peak sediment concentration during rainstorms under low mulch rates, which indicated the predominance of supply-limited conditions. However, at higher mulch rates the erosion processes were typical of a transport-limited sediment regime. The ratio of the sediment transported as primary clay to the soil matrix clay content was always less than 1, meaning that most of the clay was eroded in the form of aggregates. Transport selectivity was reflected by the silt enrichment, and silt-sized particles were transported mainly as primary particles since their effective–ultimate ratio was close to 1. The enrichment ratios for the sand-sized fractions decreased from 0.98 to 0.38 with increased mulch rates, and effective–ultimate ratios for sand-sized particles were always greater than 1, indicating that most of these particles were predominantly aggregates of finer particles, especially at high mulch rates. The findings reported in this study have important implications for the assessment and modeling of interrill erosion processes.

Abbreviations: CEC, cation exchange capacity; ER, enrichment ratio; ESP, exchangeable sodium percentage; NSLR, normalized soil loss rate; PSD, particle-size distribution; SLR, soil loss ratio.

Soil erosion by water is not only associated with on-site land degradation but also greatly contributes to negative downstream off-site impacts such as flooding, pollution, and siltation of water bodies. Soil erosion by water involves the detachment, transport, and deposition of soil materials due to the erosive forces of raindrops and runoff, and these processes are commonly divided into rill and interrill components depending on the source of eroded sediment (Meyer and Wischmeier, 1969). In regions of the world where rainfall intensities are not high, rates of interrill erosion can be considerable; even where rainfall intensities are high, interrill areas occupy a pivotal position in the erosion system, acting as links between incident rainfall and those areas of concentrated flow (rills and gullies) where most erosion occurs (Issa et al., 2006). Interrill soil erosion processes tend to be size selective, and the particle-size distribution (PSD) of eroded sediment can provide basic information regarding erosion processes (Loch and Donnollan, 1983; Miller and Baharuddin, 1987; Mitchell et al., 1983; Proffitt and Rose, 1991; Meyer et al., 1992;

Soil Sci. Soc. Am. J. 77:257–267
doi:10.2136/sssaj2012.0273
Received 28 Aug. 2012.
*Corresponding author (shizhihua70@gmail.com)

Durnford and King, 1993; Wan and EI-Swaify, 1998). Although particle-size data are available for many soils and sediments, these are commonly evaluated after sediment has been fully dispersed into its primary particles (Martinez-Mena et al., 2002). Such data may be termed the "ultimate PSD" (Slattery and Burt, 1997). In fact, eroded sediments in the field consist of both primary particles (sand, silt, and clay) and soil aggregates (Alberts et al., 1980), which constitute what can be termed the "effective PSD" (Martinez-Mena et al., 2000). A number of studies have tried to characterize eroded sediments in terms of the ultimate PSD and/or the effective PSD. However, the results have varied. Some studies reported that sediments from interrill erosion were enriched in sand at the expense of the silt- and clay-size fractions (Young and Onstad, 1978; Alberts et al., 1980). In other studies, it was observed that clay was enriched in the eroded sediment (Alberts et al., 1983). These differences in reported PSDs of eroded sediment relative to their parent soils may arise from differences in their soil properties (e.g., texture, clay content, etc.) and the conditions existing at the soil surface before a rainfall event (e.g., the condition of surface aggregates and moisture content), as well as the characteristics of the rainfall event itself (Warrington et al., 2009). Thus, information regarding both undispersed and dispersed sediment characteristics, and PSD in particular, is necessary for predicting and modeling soil erosion processes. Moreover, the relation between the effective and ultimate PSD of sediments is probably a better indicator of how the soil is detached and transported by rainfall and/or runoff (Martinez-Mena et al., 2000).

Approximately 800 million people worldwide depend directly on steeplands for their sustenance (Drees et al., 2003). Knowledge of the predominant erosion mechanisms that occur under steep slope conditions is essential if conservation measures are to be properly planned (Shi et al., 2012). Therefore, additional information on the relations between conservation measures and sediment characteristics is needed to better understand the behavior and interaction of the different factors involved in erosion processes. Mulching with vegetative residue on the soil surface is used worldwide as a soil conservation practice and is commonly used on steeplands in China (Tang, 1990). Mulch farming is a system in which a protective cover of vegetative residues, that is, straw, maize stalks, leaves, and other plant matter, is maintained on the soil surface (Smets et al., 2008). The system is particularly valuable where satisfactory plant cover cannot be established at the time of year when erosion risk is greatest (Zuazo and Plequezuelo, 2008; Smets et al., 2008). This would be in situations where a rainy season begins shortly after planting or tilling, which is the case in the dryland farming systems in China.

The effects of a mulch of vegetative residue on soil erosion have been well established through experimental investigation. Previous research has indicated that the presence of a mulch cover at the soil surface affects soil properties and the hydrologic characteristics of runoff and, therefore, soil loss by water erosion (Smets et al., 2008). Moreover, long-term mulching tends to improve soil aggregate stability and soil structure through soil protection, macrofauna activity and the incorporation of organic matter, which usually provides a high infiltration rate (Valentin and Bresson, 1992; Mulumba and Lal, 2008). Lal (1976) concluded that mulches could have beneficial effects on soil and water conservation by, for example, reducing raindrop impact, increasing water infiltration and surface storage, decreasing runoff velocity, reducing soil water evaporation, and improving both soil structure and biological activity.

Cogo et al. (1983) examined the effect of mulch cover on the size distribution of eroded sediment. They found a decrease in particle sizes with increasing cover on smooth surfaces. However, the effect of cover on particle size was negligible on rough surfaces. Gilley et al. (1986, 1987) also found that increasing residue cover usually resulted in decreased particle sizes, and that a more substantial movement of sediment in the form of aggregates occurred under the residue cover treatments. However, the PSDs of eroded sediment associated with erosion processes under various mulch rates are poorly understood. A better understanding of the sediment-size characteristics associated with different mulch rates would improve the understanding of erosion and sedimentation processes, which would improve this management practice in terms of soil and water conservation. Therefore, this study was undertaken to address the issue regarding the relations between the PSDs of eroded sediment and interrill erosion processes under various mulch rates. The specific objectives were to (i) obtain detailed information regarding the effective and ultimate PSDs of eroded sediment resulting from interrill erosion processes and (ii) investigate how mulch rates affect interrill erosion processes and sediment-size transport selectivity.

MATERIALS AND METHODS

Experimental Facilities

The experiments were conducted under simulated rainfall at the State Key Laboratory of Soil Erosion and Dryland Farming on the Loess Plateau. Rainfall intensities were adjusted by varying nozzle sizes and water pressure. Metal boxes of 2 m (length) by 1 m (width) by 0.5 m (depth) were constructed to contain the studied soil. A metal runoff collector was set at the bottom of each box to direct runoff into a container. The box could be adjusted to a desired slope of between 0° and 25°. The soil used in the experiments was a silty clay loam soil collected from Yangling in Shaanxi Province, China. Soil properties were determined by Wu et al. (2012) using standard analytical methods (Liu et al., 1996). Some properties of the soil are listed in Table 1.

Rainfall Simulation

Soil samples were air dried, crushed to pass through a 10-mm sieve and mixed thoroughly. Soil moisture was controlled to be between 10 and 12%, and the soil was packed to a depth of 30 cm in each box (in three 10-cm layers) to achieve ~1.3 g cm^{-3} bulk density. A total of 18 boxes were prepared. Additionally, each soil layer was raked lightly before the next layer was packed to reduce the discontinuity between layers. To prevent ponding of water at the lower end of the soil box, the soils were glued onto the wall of the box so that the packed soil samples were coherent with the wall. Mulch layers with 0, 15, 30, 50, 70, and 90% areal ground

cover and a thickness of 2 cm were applied, and each mulch rate was tested in triplicate. Once the boxes and their treatments were prepared, they were placed under the rainfall simulator at a slope of 15°. This slope was chosen because lands with slopes between 10° and 20° are widely used for cropping in China. The mean rainfall intensity was 85 mm h^{-1} with a range of 82 to 87 mm h^{-1} and a standard deviation of 2.7 mm h^{-1} (Zhang, 1983). A rainfall intensity of between 80 and 90 mm h^{-1} is typical of intense storms in semiarid regions of China that are dominated by monsoon climate conditions (Tang, 1990). The dynamics of rainfall were monitored using four electronic rain gauges placed around the three replicate treatments. These instruments were connected to a control data logger (CR10, Campbell Scientific, Inc., United States) operating with a 30-s time step. The duration of each rainstorm was 1 h, and deionized water (EC = 4.8 μs cm^{-1}) was used for the rainfall simulations.

For each rainfall event, runoff was volumetrically measured and sampled at 3-min intervals for sediment concentration. Collected sediment samples were allowed to settle and were then separated from the water, dried in a forced-air oven at 105°C until constant mass was achieved, and weighed. Sediment concentration of each sample was determined as the ratio of dry sediment mass to runoff volume, and soil loss was defined as the total sediment load present in the runoff water per unit area of the eroded soil surface. The soil loss ratio (SLR) was calculated as the ratio of normalized soil loss rate (NSLR) from a mulch-covered soil surface to that of an uncovered soil surface. NSLR was calculated through dividing the soil loss rate by the number of milliliters of rainfall (g m^{-2} min^{-1} mm^{-1}). To compare soil loss rates at the various mulch rates used, the SLR was calculated, and an SLR value of 1 represented the event soil loss rate from a bare soil surface. SLR was calculated using Eq. [1]:

$$SLR = \frac{NSLR_{mulch}}{NSLR_{bare}} \quad [1]$$

During rainfall events, runoff and sediment were also collected in a bucket at 3-min intervals for sediment-size measurements. The collected samples were immediately transported to the laboratory to determine the effective and ultimate particle-size distributions. The samples were first analyzed to ascertain the effective PSD of the sediment using a Malvern Mastersizer 2000 laser diffraction device (Malvern Instruments Ltd., UK). The Malvern Mastersizer 2000 has a fluid sample module and was connected to a Windows-based computer for this work. Individual samples were transferred to the fluid module that contained 1.7 L of deionized water (20°C) and were then subjected to three consecutive 1 min runs at a pump speed of 8 to 12 L min^{-1}. After determining the effective PSD of the sediment, subsamples were treated with hydrogen peroxide to remove organic matter before being dispersed overnight in sodium hexametaphosphate and were then subjected to ultrasonic dispersion. Thereafter, the ultimate PSD was also measured using the Malvern Mastersizer 2000.

Table 1. Properties of the soil used in the experiments.

Property	Unit	Value
Textural class†	(-)	Silty clay loam
Clay (<2 μm)	%	31
Fine silt (2–20 μm)	%	39
Coarse silt (20–50 μm)	%	25
Sand (>50 μm)	%	5
Bulk density	g cm^{-3}	1.32
pH (in H_2O)	(-)	8.4
Organic matter	g kg^{-1}	6
Cation exchange capacity (CEC)	$cmol_c$ kg^{-1}	17.8
$CaCO_3$ total	g kg^{-1}	56.6
Exchangeable sodium percentage (ESP)	%	0.73
Main clay minerals	(-)	Kaolinite, hydromica

† Textural class based on the USDA classification.

Calculation of Kinetic Energy Associated with Rainfall

When raindrops strike soil, the kinetic energy of the drop is transferred to soil particles and the surface water, detaching soil particles and displacing the water. Gabet and Dunne (2003) use the term 'rain power' (R, W m^{-2}) to describe the rate at which this energy is transferred to the surface. Rain power is the time derivative of the kinetic energy per unit area and was calculated in this study from

$$R = \frac{\rho I v^2 (1 - C_v) \cos\theta}{2} \quad [2]$$

where ρ is the density of water (assumed to have a constant value of 1000 kg m^{-3} at 25°C), I (m s^{-1}) is the rainfall intensity, v is the raindrop velocity (m s^{-1}), C_v represents the proportion of the area covered by straw, and θ is the slope gradient.

Calculation of Runoff Energy Associated with Mulch Rates

Stream power (Ω, W m^{-2}), which represents the energy of runoff water flowing over the soil surface, is a simple and effective predictor of soil detachment and transport (Zhang et al., 2009). If there are no rills present on the erosion surface, then Ω for the sheet flow of runoff water is given by

$$\Omega = \tau V = \rho g S q \quad [3]$$

where τ is the shear stress, V is the mean flow velocity (m s^{-1}), ρ is the density of water (assumed to have a constant value of 1000 kg m^{-3} at 25°C), g is the gravitational acceleration (9.8 m s^{-2}), S is the sine of the erosion surface slope, and q is the unit width flow discharge rate (m^3 m^{-2} s^{-1}).

Some or all of the stream power is available to remove and transport soil particles from the erosion surface. The mulch absorbs a portion of the runoff shear stress that is normally borne by the soil. Therefore, the shear stress (τ) presented in Eq. [3] can be split into two portions (Prosser et al., 1995): τ_s, the shear stress on the soil, and τ_c, the shear stress on the mulch. The fraction of the shear stress exerted on bare soil (τ_s/τ) may be a function of the uncovered portion of the soil surface, that is, $(1-C_v)$. However, because the mulches not only shield the portion of soil that is

Table 2. Rainfall simulation results under various mulch rates.†

Mulch rate	Rainfall intensity	Steady r6unoff rate	Runoff coefficient	Sediment concentration	Soil loss rate	Soil loss ratio (SLR)
%	mm h^{-1}	mm h^{-1}	%	g L^{-1}	g m^{-2} min^{-1}	
0	82.2	74.3a	82.9a	12.5a	15.9a	1
15	82.8	68.2ab	72.4b	8.7b	8.0b	0.50
30	85.2	61.6b	62.4c	5.2c	6.6c	0.43
50	84.0	45.2c	47.7d	4.5c	5.9c	0.40
70	85.3	26.8d	14.1e	3.1d	1.7d	0.10
90	86.9	18.2e	11.4e	2.0e	0.7e	0.04

† Means in a column followed by the same letter are not significantly different at $P < 0.05$. Each value of sediment concentration represents the mean value.

bare but also reduce velocity and shear stress in the boundary layer, such a function is probably nonlinear. The following relation is assumed (Siepel et al., 2002):

$$\tau_s/\tau = (1\text{-}C_v)^p \quad [4]$$

where p is a calibrating parameter. Equation [4] is substituted into Eq. [3] to obtain the actual stream power (Ω_m) required to remove and transport soil particles:

$$\Omega_m = \rho g S q\,(1\text{-}\,C_v)^p \quad [5]$$

The value $p = 1.76$ was adopted in this study (Eq. [5]) based on calibrating the model with measured data; for this calibration, we employed the approach proposed by Siepel et al. (2002).

Data Analyses

Data analyses included regression, determining correlations, and ANOVA testing. Assumptions of normality and the homogeneity of variances were tested using the Shapiro–Wilk and Brown–Forsyth tests, respectively. Because some variables did not satisfy these assumptions, alternative nonparametric tests were used to compare multiple independent groups of samples (Kruskall–Wallis ANOVA). When the ANOVA null hypothesis was rejected, post hoc pairwise comparisons (the Bonferroni test) were performed to investigate differences between pairs of means. All tests were performed using the statistical program SPSS 17.0.

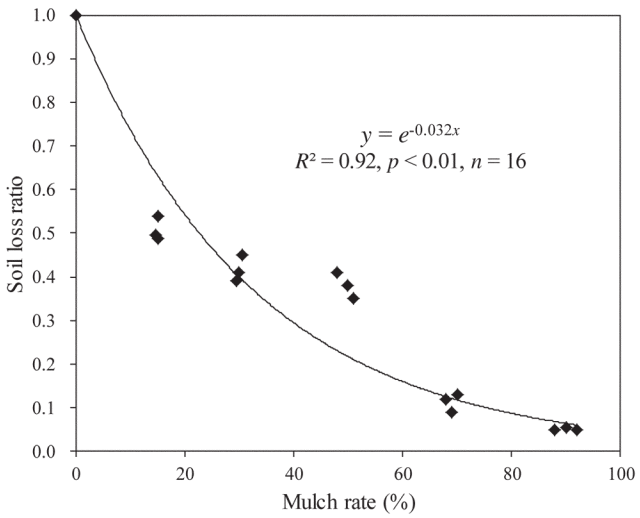

Fig. 1. The relation between soil loss ratio and mulch rate.

RESULTS AND DISCUSSION

Runoff and Soil Loss

The presence of mulch rates influenced runoff as shown by the runoff coefficients and the steady state runoff rates (Table 2). The runoff coefficient, defined as the percentage of rainfall converted into overland flow during an event, consistently decreased with increasing mulch rate. Mulch rates of 15, 30, 50, 70, and 90% reduced the runoff coefficient values when compared with the bare soil case by 10.5, 20.5, 35.2, 68.8, and 71.5%, respectively. The steady-state runoff rate varied in the same manner with a rate of 74.3 mm h^{-1} for the bare soil, which decreased with increasing mulch cover to 18.2 mm h^{-1} for the 90% mulch rate. Similar to runoff, soil loss decreased with increasing mulch rate. Low mulch rates greatly reduced erosion, and the soil loss rate for the 15% mulch rate was reduced by half compared with the bare soil (15.9 and 8.0 g m^{-2} min^{-1}, respectively). The reduced thin-flow velocity due to mulching accounted for much of the observed decrease in soil erosion (Poesen and Lavee, 1991). However, a substantial reduction in soil loss occurred for the 70% mulch rate when soil loss was reduced to 10.7% of that observed when using no mulch; a 90% mulch rate reduced soil loss to less than 5% of the bare soil losses. The Bonferroni test separated sediment concentration values into five groups ($P < 0.01$; Table 2) but did not detect significant differences between the values for the mulch rates of 30 and 50%. The relation between SLR and mulch rate was best described by an exponential function ($R^2 = 0.92$; Fig. 1).

Temporal Runoff and Sediment Response to Mulch Rates

Figure 2 illustrates the temporal variation in runoff rate and sediment concentration under various mulch rates. Runoff initiation was delayed as the mulch rate increased. The cumulative rainfall levels required to start runoff were 4.1, 5.5, 7.3, 11.2, 16.3, and 18.1 mm for the 0, 15, 30, 50, 70, and 90% mulch rates, respectively. The bare soil and low mulch rates (15 and 30%) exhibited similar runoff processes and patterns, although the runoff rates and runoff coefficients of the mulched soils were significantly lower than those of the bare soil (Table 2 and Fig. 2a). For the mulch rates of 70 and 90%, the runoff rate slowly increased during the first 45 to 50 min, and the steady state was reached after 75 mm of cumulative rainfall. Therefore, runoff depended largely on the applied mulch rates. The mulch layer on the soil surface contributed to providing initial protection against surface sealing induced by raindrop impact, thereby increasing infiltration (Jordan et al.,

2010). Moreover, porous media can store liquid water (Savabi and Stott, 1994).

Sediment concentration exhibited a different dependence on the mulch rate (Fig. 2b). The bare soil and 15% mulch rate produced high sediment concentrations during the first few minutes of runoff. The sediment concentrations then decreased to a constant level, and this decrease was accompanied by increasing runoff rates. In contrast, 70 and 90% mulch rates led to increasing sediment concentrations and runoff rates until both became more or less constant (Fig. 2b). Maximum sediment concentrations occurred at the same time as the peak discharges. For the mulch rates of 30 and 50%, sediment concentrations declined slightly (approximately by 2–4 g L^{-1}) with time and varied over a narrow range (generally 4–8 g L^{-1}) during the rainstorms. The relation between sediment yield rate and runoff rate as an indicator of soil erodibility has commonly been regarded as a linear function under net detachment conditions or as a quadratic regression under depositional conditions (Huang and Bradford, 1993). In this study net detachment conditions were always the case. Therefore, the relation was regressed using the following linear equation:

$$Q_s = aQ_w + b \quad [6]$$

where Q_s is the sediment yield rate (g m^{-2} min^{-1}), Q_w is the runoff rate (mm min^{-1}), a is a regression coefficient (g m^{-2} mm^{-1}) describing soil erodibility, and b is also a regression coefficient (g m^{-2} min^{-1}). The slopes of the regression lines differed significantly among different mulch rates (Table 3).

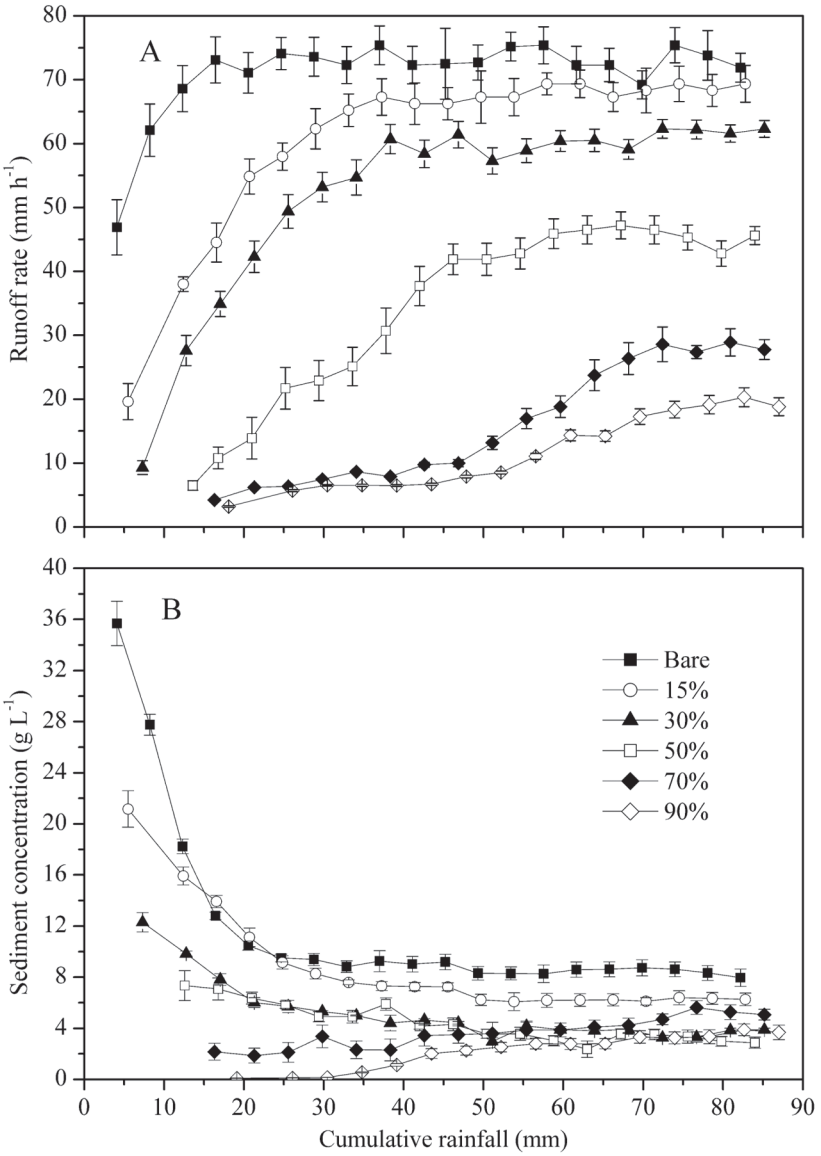

Fig. 2. The temporal variation in the (a) runoff rate and (b) sediment concentration under various mulch rates.

The relations between Q_s and Q_w could be divided into two distinct linear types: lower mulch rates (≤30%), where Q_w was negatively correlated with Q_s with a negative erodibility (a value), and higher mulch rates (≥50%), where Q_s increased with Q_w, resulting in a positive relation. The absolute values of the linear slopes, that is, soil erodibility, ranged from –55.50 g m^{-2} mm^{-1} for the bare soil to 10.16 g m^{-2} mm^{-1} for the 90% mulch rate (Table 3). The change in soil erodibility with increasing mulch rates could be attributed to an increase in soil surface roughness and decreases in effective raindrop kinetic energy and flow velocity with increasing cover, which led to transport-limited (negative a value) or detachment-limited (positive a value) conditions. The components of the mulch increased soil surface roughness and acted as successive barriers that obstructed

Table 3. The slope (*a*), intercept (*b*), and coefficient of determination (R^2) of the linear regression of sediment yield rate (Q_s) and runoff rate (Q_w) ($Q_s = aQ_w + b$) for various mulch rates.

Mulch rates (%)	*a*	95% Confidence interval of *a*		*b*	*n*	R^2
		Lower limits	Upper limits			
0	–55.50	–71.04	–39.96	90.02	60	0.469**
15	–13.39	–17.27	–9.51	30.31	57	0.465**
30	–5.39	–7.01	–3.78	14.18	57	0.450**
50	8.24	6.65	9.83	–0.31	54	0.677**
70	9.28	7.81	10.86	–0.46	51	0.712**
90	10.16	8.98	11.34	–0.98	48	0.814**

**Significant at $P < 0.01$.

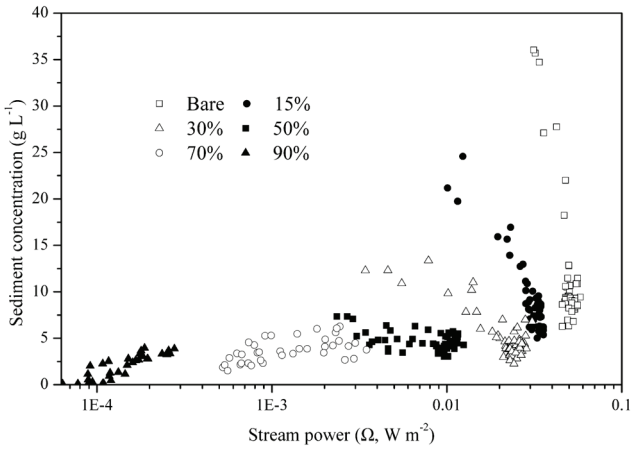

Fig. 3. Instantaneous stream power versus sediment concentration for various mulch rates.

runoff (GiMey et al., 1991). Consequently, runoff pathways were generally more tortuous, and runoff flow velocity was generally lower for mulched soils (Poesen and Lavee, 1991). Therefore, soil erosion was markedly reduced under high mulch rates because detachment by runoff and rainfall was diminished and soil infiltration rates were increased.

To aid in further interpretation of the experimental results, we explored the relation between instantaneous stream power and sediment concentration to identify the dominant erosive processes involved (Fig. 3). At high mulch rates (70 and 90%), a positive linear relation existed between stream power and sediment concentration. The increase in sediment concentration with stream power indicated that the erosion process was characterized by a transport-limited sediment regime. This regime might include raindrop detachment followed by raindrop-induced flow transport, as suggested by Kinnell (2005, 2012); such a system is always transport-limited. However, for lower mulch rates (≤30%) the increased stream power did not increase sediment concentration, indicating a lack of flow detachment under these conditions. The negative linear trend between sediment concentration and stream power indicated a reduction in soil erodibility with time, which suggested the existence of a detachment-limited condition at low mulch rates (Durnford and King, 1993). The fact that the stream power did not reach a maximum at the same time as the sediment concentration in runs under low mulch rates emphasized the predominance of supply-limited conditions.

Effects of Mulch Rates on the Effective Particle-Size Distribution of Sediment

The effective sediment sizes were classified as clay-sized (<2 μm), fine silt-sized (2–20 μm), coarse silt-sized (20–50 μm) and sand-sized (>50 μm) (Martinez-Mena et al., 2002). Figure 4 illustrates the temporal variations in the relative proportion of the effective PSD of eroded sediment under the six mulch rates.

Despite the studied soil having a clay content of 31%, only 11 to 19% (generally 13–16%) of the total sediment consisted of clay-sized particles. The percentage of clay-sized sediment decreased slightly, by approximately 2 to 4%, with the cumulative increase in rainfall for all the treatments. These data suggested that relatively little clay dispersion occurred and that most of the clay in the sediments was present in the form of aggregates. Furthermore, partly dispersed clay would likely enter the soil pore system as part of the sealing process leading to depletion of clay-sized particles (Fox and Le Bissonnais, 1998). Clay-sized particles in soils are commonly associated with aggregation by rearrangement and flocculation (Bronick and Lal, 2005). The content of clay-sized sediment in runoff provides an indication of the forces that acted on the aggregates during detachment and transport by the erosive agent (Loch and Donnollan, 1983). Le Bissonnais (1996) identified four main mechanisms responsible for aggregate breakdown: slaking, physicochemical dispersion, differential swelling, and mechanical breakdown. The type of breakdown mechanism present affects the degree of aggregate breakdown and the size distribution of soil fragments available for detachment and transport. The soil used in the experiments exhibited very low exchangeable sodium percentage (ESP) (0.73%), and its main clay minerals were kaolinite and hydromica (Table 1). Physico-chemical dispersion results from the reduction of the attractive forces between colloidal particles while wetting, which depends largely on the ESP of the soil, while breakdown by differential swelling increases with increasing clay content. Slaking involves compression of entrapped air during wetting that destructively explodes from within an aggregate, while mechanical breakdown mainly results from raindrop impact because thin-flow energy is expected to be low relative to that of raindrop impacts (Shi et al., 2012). Therefore, the main mechanisms of aggregate breakdown during water erosion are slaking and mechanical breakdown (Le Bissonnais, 1996).

As shown in Fig. 5, the percentage of clay-sized particles in the sediment was significantly correlated with the instantaneous rain power. The relation could be fitted to the following exponential equation: $y = \alpha + \beta e^{\bar{\omega} x}$. In this equation, the constant α was controlled by the slaking mechanisms of aggregate breakdown, which were determined by the soil properties and antecedent moisture content (Le Bissonnais, 1996). In our experiment, the percentage of eroded clay-sized particles decreased with increasing mulch rates. This finding could be attributed largely to the differences in the impact of raindrops onto bare soil or onto soil covered with straw mulch. Straw mulch partially intercepted the raindrops and absorbed the raindrop energy dependent on the mulch cover (Savabi and Stott, 1994; Adekalu et al., 2006).

The fraction of sand-sized sediment decreased with time under low mulch rates (<30%) because of a source limited process but increased under high mulch rates (>70%) resulting from a transport limited process. Sand-sized sediment also significantly fluctuated with decreasing mulch rates. The coefficients of variation were 13.3, 7.3, 8.5, 5.8, 2.9, and 3.6% for the bare soil and the 15, 30, 50, 70, and 90% mulch rates, respectively. The sediment was principally composed of silt-sized sediment, which accounted for approximately 60 to 80% of the sediment load (Fig. 4). There appeared to be an implied silt enrichment of the sediment in relation to the parent soil. Young (1980) suggested

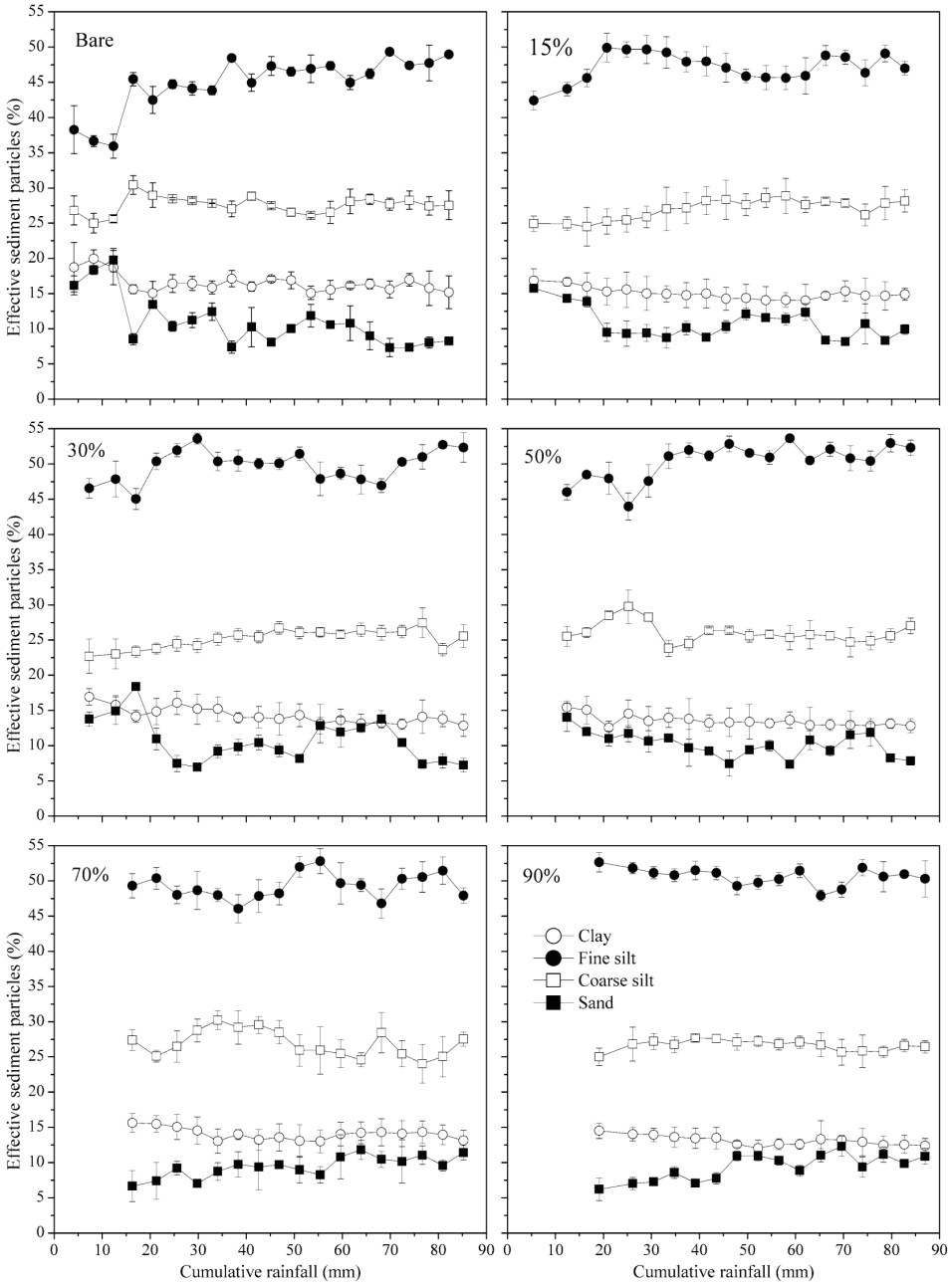

Fig. 4. Changes in the percentage of effective sediment particles with cumulative rainfall for various mulch rates.

that soils with silt contents of greater than 33% usually generated sediments in the silt-size range. He postulated that larger particles have had sufficient mass to limit their movement, but while cohesive forces impeded particle detachment for of clay-sized particles. According to Young (1980), soil texture was the main factor behind causing differences in sediment-size distributions. However, the results obtained by Durnford and King (1993) revealed that when rainfall energy was sufficiently high to break soil aggregates apart, clay became available for transport. The relative proportions of the different size classes thereby depend on both rainfall and runoff properties. These conclusions may not necessarily be contradicted by our results, since any differences may rather reflect the different combinations of rainfall energy,

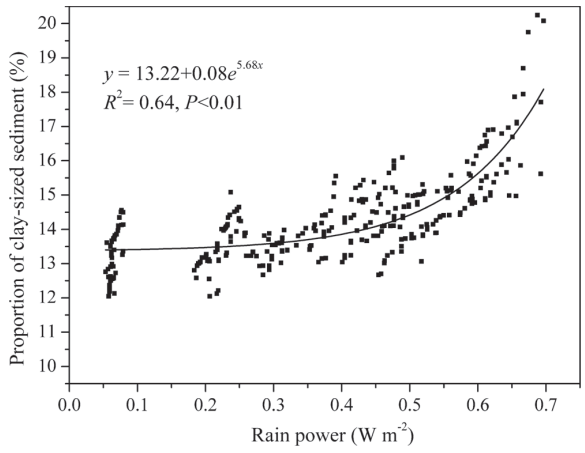

Fig. 5. The relation between rain power and the percentage of clay-sized particles in sediment.

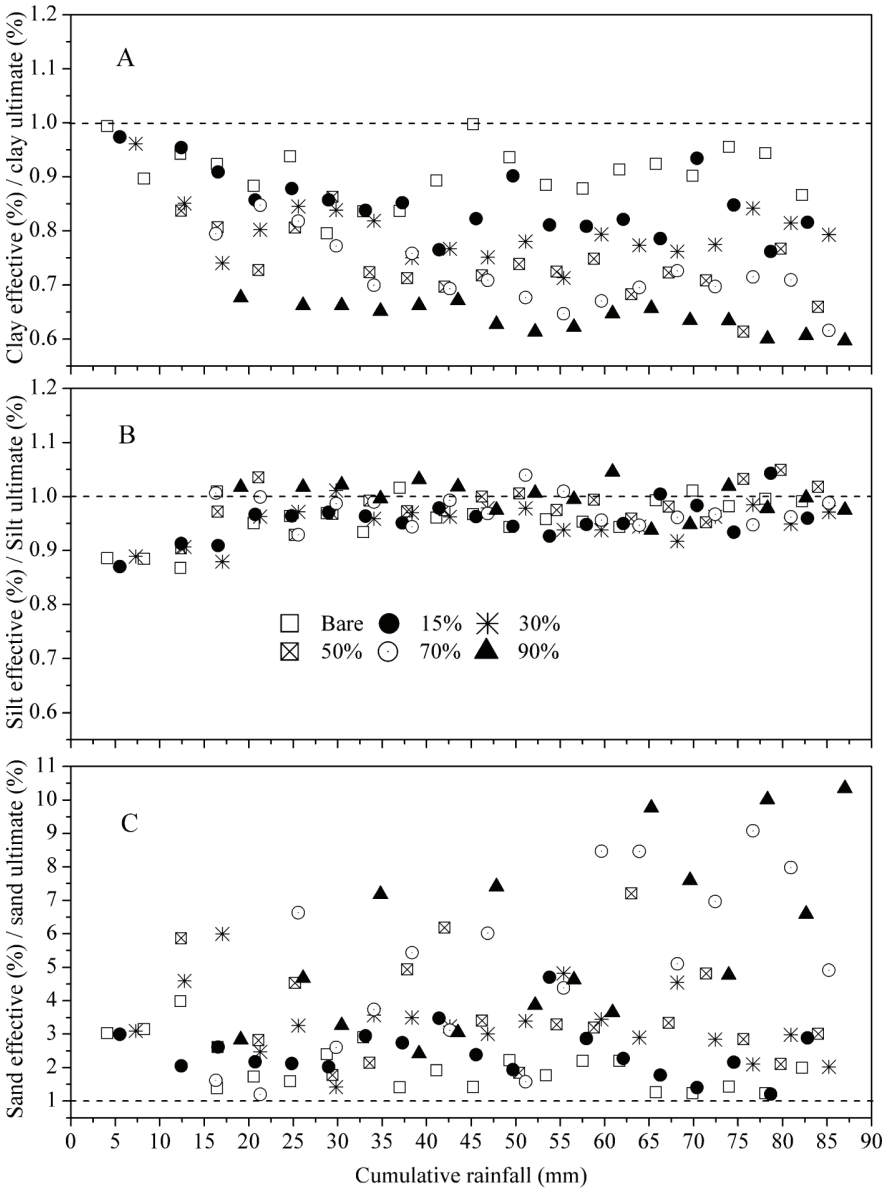

Fig. 6. Comparison of the effective–ultimate ratios in the clay, silt and sand fractions for various mulch rates (note the different scale on the *y* axis for sand-sized particles).

runoff energy and soil surface characteristics under investigation in these studies (Le Bissonnais et al., 2005).

The Effects of Mulch Rates on Transport Selectivity

The relative proportion of the effective and ultimate PSDs of the sediment can act as an indicator of how the different fractions are eroded and transported by the flow (Martinez-Mena et al., 2002). An effective–ultimate ratio of 1 indicates particle disaggregation by slaking and mechanical breakdown and the transport of the sediment as primary particles. A ratio greater than 1 suggests that these sediment particles can be disaggregated and are therefore transported as aggregates rather than as primary particles. Figure 6 illustrates the temporal variation in the effective–ultimate ratios for clay-, silt-, and sand-sized particles.

The silt-sized sediments were usually transported as primary particles, as reflected by their mean effective–ultimate ratios being close to 1 (Table 4) and fluctuating around a value of approximately 1 most of the time (Fig. 6b). The effective–ultimate ratios of the clay-sized sediments were always less than 1 and exhibited a slight decrease with time (Fig. 6a). Furthermore, the 15, 30, 50, 70, and 90% mulch rates resulted in significant reductions in the effective–ultimate ratios of the clay-sized sediments over those from the bare soil by 5.3, 12.5, 19.3, 20.9, and 29.9%, respectively (Table 4). The effective–ultimate ratios for sand-sized particles were always greater than 1 (Fig. 6c), indicating that most of these particles were predominantly aggregates of finer particles. Greater mulch rates resulted in increased effective–ultimate ratios, and the mean value of the ratio was 2.75-fold lower for the bare soil than for the 90% mulch rate.

Comparison of the ultimate PSD of the eroded sediment with that of the original soil also provides a measure of the particle-size selectivity of sediment mobilization (Martinez-Mena et al., 2000). The enrichment ratio (ER) is given by

$$\mathrm{ER}=\frac{\text{percentage of particles in a given size class in eroded sediment}}{\text{percentage of particles in a given size class in original soil}} \quad [7]$$

An ER greater than 1 reflects enrichment where a given particle-size class constitutes a greater proportion of the eroded sediment than of the original soil. An ER less than 1 represents depletion where a given size class constitutes a greater proportion of the original soil than of the eroded sediment. Enrichment ratios were calculated by comparing the percentage of clay-, silt-, and sand-sized sediment classes to those of the silty clay loam soil matrix, which was composed of 31% clay, 64% silt, and 5% sand (Fig. 7).

Table 4. Mean values of the effective–ultimate ratios of the clay, silt, and sand fractions for various mulch rates.†

Mulch rates, %	0	15	30	50	70	90
Clay-size particles	0.912a	0.864b	0.798c	0.736d	0.722d	0.639e
Silt-size particles	0.955a	0.953a	0.949a	0.984b	0.976ab	0.992b
Sand-size particles	1.992a	2.462ab	3.325bc	3.661c	5.136d	5.470d

† Means in the same row followed by the same letter are not significantly different at $P < 0.05$.

Transport selectivity was reflected by the silt enrichment with mean values of 1.26, 1.28, 1.31, 1.31, 1.30, and 1.33 for the 0, 15, 30, 50, 70, and 90% mulch rates, respectively. The ratio of the sediment transported as primary clay to the clay of the soil matrix was never greater than 1, meaning that most of the clay was eroded in the form of aggregates, especially at high mulch rates, which led to larger aggregates being eroded. The PSD of the larger aggregates were not necessarily proportional to the primary PSD of the soil matrix (Young, 1980; Nicholas and Walling, 1996). Increasing mulch cover reduced aggregate breakdown because of the interception of raindrops by mulch on the soil surface (Savabi and Stott, 1994). As the mulch rate increased from 0 to 90%, enrichment ratios for the sand-sized fractions decreased from 0.98 to 0.38, and the differences between mulch rates were significant ($F = 55.1$, $P < 0.01$). Increasing the mulch rate reduced the energy available for detachment and transport by rainfall and runoff, as well as by reducing the degree of aggregate breakdown, which led to the increased movement of aggregates relative to the equivalent sand-size primary particles due to the former's lower density.

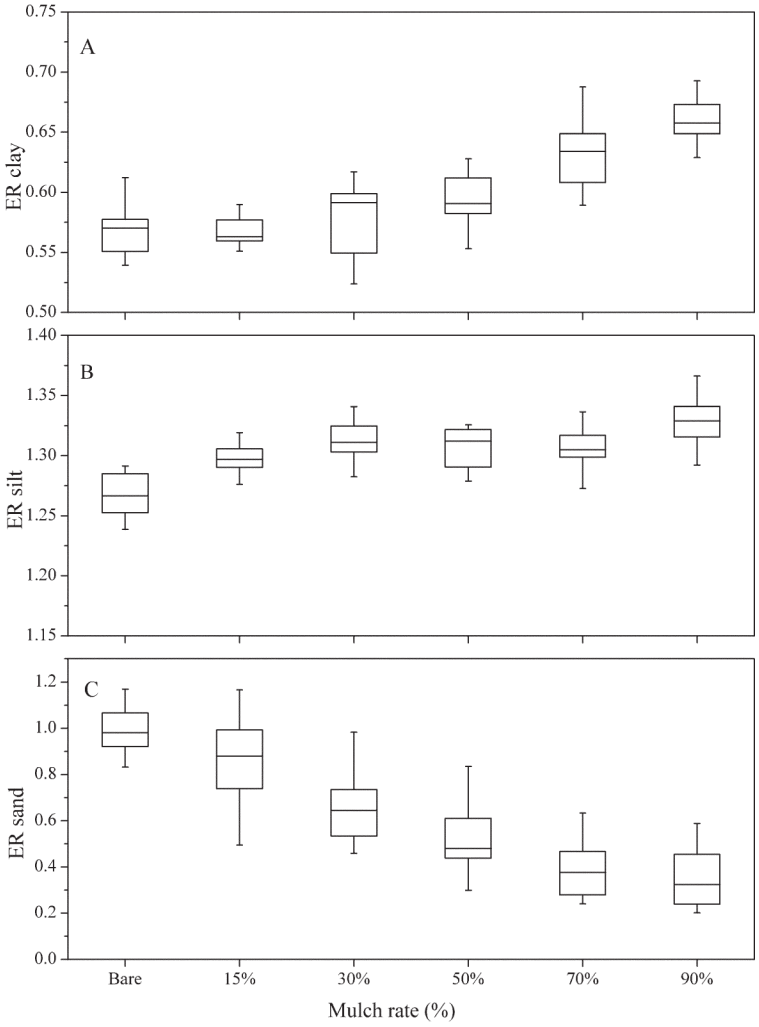

Fig. 7. Box plots of the enrichment ratio (ER) of the ultimate (a) clay, (b) silt, and (c) sand for various mulch rates (note the different scale on the *y* axis).

Comparison of Measured Sediment Concentration with Theory

There are a number of reported size-selective erosion models (e.g., Hairsine and Rose, 1991, 1992; De Roo et al., 1996; Flanagan and Nearing, 2000). The theory developed by Hairsine and Rose (1992) treated erosion and deposition processes independently, with the net outcome being the difference between these two process groups. The Hairsine–Rose theory has been successfully applied within GUEST (Griffith University Erosion System Template). From Hairsine and Rose (1992), the sediment concentration at the transport limit (Ct) is given by:

$$C_t = \frac{F(\Omega - \Omega_0)}{v_{av} g D}\left(\frac{\sigma}{\sigma - \rho}\right) \quad [8]$$

where F is the fraction of stream power effective in erosion, which generally approximates to 0.1, σ is the wet sediment density, ρ is the density of the fluid, Ω is the stream power with a threshold value Ω_0, D is the flow depth, and v_{av} is the mean settling velocity of the sediment.

Neglecting the threshold stream power for erosion commencement, Fig. 8 compares values of C_t predicted by Eq. [8] with measured sediment concentrations. Figure 8 shows good agreement between measured and predicted sediment concentrations when these were lower but increasing divergence from the 1:1 relation as sediment concentration increased. As shown in Fig. 3, increased sediment concentration did not always correspond to an increase in stream power, and similarly the increased divergence shown in Fig. 8 did not always correspond to increased stream power. Approximate (Rose et al., 2007) and

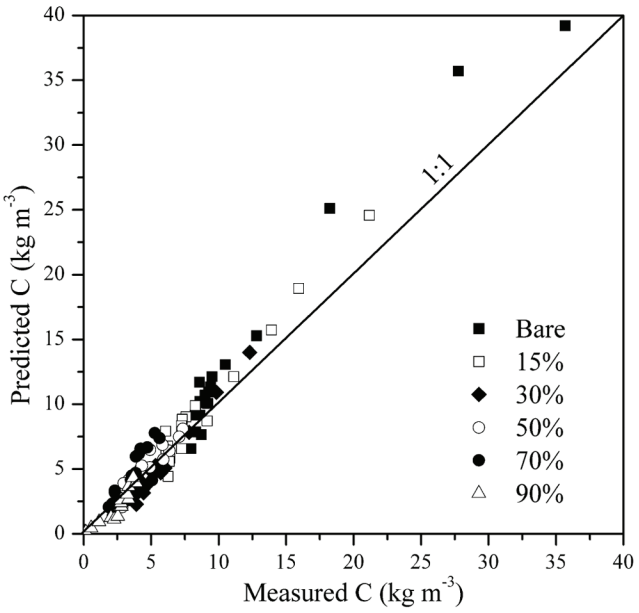

Fig. 8. Comparison of measured sediment concentration with that predicted using Eq. [8] for various mulch rates.

analytic (Tromp-van Meerveld et al., 2008) solutions for the Hairsine–Rose theory (Hairsine and Rose, 1991, 1992) for flow and rainfall erosion, respectively, have shown some differences between observations and predictions. The differences resulted from the mechanisms of entrainment and transportation of soil particles by surface runoff. Total soil loss was the sum of saltation–suspension and bed load transport mechanisms, such as rolling or mass movement (Asadi et al., 2011). With increasing stream power on steeper slopes, bed-load transport by rolling of the large-sized sediment particles became an increasingly important transport mechanism (Shi et al., 2012). The presence of rolling in conjunction with or parallel to saltation–suspension, the only mechanisms assumed in the theory, has been suggested as a possible reason for such differences (Rose et al., 2007; Asadi et al., 2011). Saltation–suspension would be expected to be a more efficient transport mechanism than bed load transport mechanisms such as rolling or mass movement. Thus, if bed load transport became a more important mechanism at higher stream powers, then a corresponding increased overestimation of sediment concentration by Eq. [8] would be expected.

Understanding the effect of mulches on water erosion is of practical significance in properly managing the use of straw mulch on land in semiarid regions. The influence of more types of organic mulches (such as straw, leaves, stalks, wood, or bark chips) and mulch-layer thickness on water erosion still needs more intensive investigation. The findings in this study also stress the importance of studying the effective sediment PSD (as well as the ultimate PSD) because the use of primary grain-size data in transport mechanisms could produce erroneous results since substantial quantities of clay are often transported in aggregated form. This is also significant in regard to nutrient transport because nutrients move like aggregates and are, thus, less likely to be transported (Loch and Donnollan, 1983).

CONCLUSIONS

The processes of runoff and sediment generation under straw mulch were studied with different cover levels (0, 15, 30, 50, 70, and 90%) on a slope of 15° under simulated rainfall. We analyzed (i) the effective and ultimate PSDs of sediments using laser diffraction and (ii) the effect of rain power, stream power, and mulch rates on runoff, sediment yield, and sediment PSD. Compared with the bare soil, the increasing mulch rates decreased the mean runoff rate by 12.7 to 86.6% and the steady runoff rate by 8.2 to 75.5%. Mulch played a more important role in reducing soil loss than runoff. The erosion rate was reduced by 49.9 to 95.6% under mulch when compared with the bare soil. The fact that the maximum stream power did not occur at the same time as the peak sediment concentration for low mulch rates emphasized the predominance of supply-limited conditions. Under high mulch rates, maximum sediment concentration occurred at the same time as the peak discharge, and the erosion process was characterized by a transport-limited sediment regime. The percentage of clay-sized sediment decreased with increasing rainfall duration and mulch rate. The effective–ultimate ratio of this sediment was always less than 1 and decreased with increasing mulch rate. The sediment was principally composed of silt-sized sediment, which was mainly transported as primary particles due to its effective–ultimate ratio of close to 1. The amount of sand-sized sediment decreased with time under low mulch rates but increased with time under high mulch rates. Sand-sized sediment was mainly transported as aggregates, and the effective–ultimate ratio increased with mulch rate. A major influence of mulch rate on interrill erosion and dynamic changes in the PSD appeared to be exerted through its impact on complex combinations of rainfall energy, runoff energy, and soil surface characteristics. Sediment concentrations predicted using the Hairsine–Rose theory, which assumed the dominance of saltation–suspension, were compared with measured concentrations. This comparison indicated that bed load transport, such as rolling or mass movement, became an important transport mechanism with increasing stream power on steeper slopes. Our results indicated that any attempt to elucidate the dynamics of soil loss from interrill areas must consider the potential contrast between the effective and ultimate PSDs of the sediment in response to aggregation.

ACKNOWLEDGMENTS

Financial support for this research was provided by the National Natural Science Foundation of China (41271296), the Program for New Century Excellent Talents in University (NCET-10-0423), and the Fundamental Research Funds for the Central Universities (2011PY001).

REFERENCES

Adekalu, K.Q., D.A. Okunada, and J.A. Osunbitan. 2006. Compaction and mulching effect on soil loss and runoff from two southwestern Nigeria agricultural soils. Geoderma 137:226–230. doi:10.1016/j.geoderma.2006.08.012

Alberts, E.E., W.C. Moldenhauer, and G.R. Foster. 1980. Soil aggregates and primary particles transported in rill and interrill flow. Soil Sci. Soc. Am. J. 44:590–595. doi:10.2136/sssaj1980.03615995004400030032x

Alberts, E.E., R.C. Wendt, and R.F. Piest. 1983. Physical and chemical properties of eroded soil aggregates. Trans. ASAE 26:465–471.

Asadi, H., A. Moussavi, H. Ghadiri, and C.W. Rose. 2011. Flow-driven soil erosion processes and the size selectivity of sediment. J. Hydrol. 406:73–81. doi:10.1016/j.jhydrol.2011.06.010

Bronick, C.J., and R. Lal. 2005. Soil structure and management: A review. Geoderma 124:3–22. doi:10.1016/j.geoderma.2004.03.005

Cogo, N.P., W.C. Moldenhauer, and G.R. Foster. 1983. Effect of crop residue, tillage-induced roughness and runoff velocity on size distribution of eroded soil aggregates. Soil Sci. Soc. Am. J. 47:1005–1008. doi:10.2136/sssaj1983.03615995004700050033x

De Roo, A.P.J., C.G. Wesseling, and C.J. Ritsema. 1996. LISEM: A single-event physically based hydrological and soil erosion model for drainage basins. I: Theory, input and output. Hydrol. Processes 10:1107–1117. doi:10.1002/(SICI)1099-1085(199608)10:8<1107::AID-HYP415>3.0.CO;2-4

Drees, L.R., L.P. Wilding, P.R. Owens, B. Wu, H. Perottoa, and H. Sierra. 2003. Steepland resources: Characteristics, stability and micromorphology. Catena 54:619–636. doi:10.1016/S0341-8162(03)00138-3

Durnford, D., and P. King. 1993. Experimental study of processes and particle-size distributions of eroded soil. J. Irrig. Drain. Eng. 119:383–398. doi:10.1061/(ASCE)0733-9437(1993)119:2(383)

Flanagan, D.C., and M.A. Nearing. 2000. Sediment particle sorting on hillslope profiles in the WEPP model. Trans. ASAE 43:573–583.

Fox, D., and Y. Le Bissonnais. 1998. Process-based analysis of aggregate stability effects on sealing, infiltration, and interrill erosion. Soil Sci. Soc. Am. J. 62:717–724. doi:10.2136/sssaj1998.03615995006200030025x

Gabet, E.J., and T. Dunne. 2003. Sediment detachment by rain power. Water Resour. Res. 39:1002, doi:10.1029/2001WR000656

Gilley, J.E., S.C. Finkner, R.G. Spomer, and L.N. Mielke. 1986. Size distribution of sediment as affected by corn residue. Trans. ASAE 29:1273–1277.

Gilley, J.E., S.C. Finkner, and G.E. Varvel. 1987. Size distribution of sediment as affected by surface residue and slope length. Trans. ASAE 30:1419–1424.

GiMey, J.E., E.R. Kottwitz, and G.A. Wieman. 1991. Roughness coefficients for selected residue materials. J. Irrig. Drain. Eng. 117:503–514. doi:10.1061/(ASCE)0733-9437(1991)117:4(503)

Hairsine, P.B., and C.W. Rose. 1991. Rainfall detachment and deposition: Sediment transport in the absence of flow-driven processes. Soil Sci. Soc. Am. J. 55:320–324. doi:10.2136/sssaj1991.03615995005500020003x

Hairsine, P.B., and C.W. Rose. 1992. Modeling water erosion due to overland flow using physical principles: 1. Sheet flow. Water Resour. Res. 28:237–243. doi:10.1029/91WR02380

Huang, C.H., and J.M. Bradford. 1993. Analyses of slope and runoff factors based on the WEPP erosion model. Soil Sci. Soc. Am. J. 57:1176–1183. doi:10.2136/sssaj1993.03615995005700050002x

Issa, O. M., Y. Le Bissonnais, O. Planchon, D. Favis-Mortlock, N. Silvera, and J. Wainwright. 2006. Soil detachment and transport on field- and laboratory-scale interill areas: Erosion processes and the size-selectivity of eroded sediment. Earth Surf. Process. Landf. 31:929–939. doi:10.1002/esp.1303

Jordan, A., L.M. Zavala, and J. Gil. 2010. Effects of mulching on soil physical properties and runoff under semi-arid conditions in southern Spain. Catena 81:77–85. doi:10.1016/j.catena.2010.01.007

Kinnell, P.I.A. 2005. Raindrop impact induced erosion processes and prediction: A review. Hydrol. Processes 19:2815–2844. doi:10.1002/hyp.5788

Kinnell, P.I.A. 2012. Modeling of the effect of flow depth on sediment discharged by rain-impacted flows from sheet and interrill erosion areas: A review. Hydrol. Processes. 10.1002/hyp.9363.

Lal, R. 1976. Soil erosion problems on an Alfisol in Western Nigeria and their control: Mulching effect on runoff and soil loss. I.T.A. Monogr. 1. Int. Inst. for Tropical Agric., Ibadan, Nigeria.

Le Bissonnais, Y. 1996. Aggregate stability and assessment of soil crustability and erodibility: I. Theory and methodology. Eur. J. Soil Sci. 47:425–437. doi:10.1111/j.1365-2389.1996.tb01843.x

Le Bissonnais, Y., O. Cerdan, V. Lecomte, H. Benkhadra, V. Souchère, and P. Martin. 2005. Variability of soil surface characteristics influencing runoff and interrill erosion. Catena 62:111–124. doi:10.1016/j.catena.2005.05.001

Liu, G.S., N.H. Jiang, and L.D. Zhang. 1996. Soil physical and chemical analysis and description of soil profiles (in Chinese). Standards Press of China, Beijing.

Loch, R.J., and T.E. Donnollan. 1983. Field rainfall simulator studies on two clay soils of the Darling downs, Queensland. II Aggregate breakdown, sediment properties and soil erodibility. Aust. J. Soil Res. 21:47–58. doi:10.1071/SR9830047

Martinez-Mena, M., R.J. Alvarez, J. Albaladejo, and V.M. Castillo. 2000. Influence of vegetal cover on sediment particle size distribution in natural rainfall conditions in a semiarid environment. Catena 38:175–190. doi:10.1016/S0341-8162(99)00073-9

Martinez-Mena, M., V. Castillo, and J. Albaladejo. 2002. Relations between interrill erosion processes and sediment particle size distribution in a semiarid Mediterranean area of SE of Spain. Geomorphology 45:261–275. doi:10.1016/S0169-555X(01)00158-1

Meyer, L.D., D.E. Line, and W.C. Harmon. 1992. Size characteristics of sediment from agricultural soils. J. Soil Water Conserv. 47:107–111.

Meyer, L.D., and W.H. Wischmeier. 1969. Mathematical simulation of the process of soil erosion by water. Trans. ASAE 12:754–758, 762.

Miller, W.P., and M.K. Baharuddin. 1987. Particle size of interrill-eroded sediments from highly weathered soils. Soil Sci. Soc. Am. J. 51:1610–1615. doi:10.2136/sssaj1987.03615995005100060037x

Mitchell, J.K., S. Mostaghimi, and M. Pound. 1983. Primary particle and aggregate size distribution of eroded soil from sequenced rainfall events. Trans. ASAE 26:1773–1777.

Mulumba, L.N., and R. Lal. 2008. Mulching effects on selected soil physical properties. Soil Tillage Res. 98:106–111. doi:10.1016/j.still.2007.10.011

Nicholas, A.P., and D.E. Walling. 1996. The significance of particle aggregation in the overbank deposition of suspended sediment on river floodplains. J. Hydrol. 186:275–293. doi:10.1016/S0022-1694(96)03023-5

Poesen, J., and H. Lavee. 1991. Effects of size and incorporation of synthetic mulch on runoff and sediment yield from interills in a laboratory study with simulated rainfall. Soil Tillage Res. 21:209–223. doi:10.1016/0167-1987(91)90021-O

Proffitt, A.P.B., and C.W. Rose. 1991. Soil erosion processes: II. Settling velocity characteristics of eroded sediment. Aust. J. Soil Res. 29:685–695. doi:10.1071/SR9910685

Prosser, I.P., W.E. Dietrich, and J. Stevenson. 1995. Flow resistance and sediment transport by concentrated overland-flow in a grassland valley. Geomorphology 13:71–86. doi:10.1016/0169-555X(95)00020-6

Rose, C.W., B. Yu, H. Ghadiri, H. Asadi, J.Y. Parlange, W.L. Hogarth, and J. Hussein. 2007. Dynamic erosion of soil in steady sheet flow. J. Hydrol. 333:449–458. doi:10.1016/j.jhydrol.2006.09.016

Savabi, M., and D. Stott. 1994. Plant residue impact on rainfall interception. Trans. ASAE 37:1093–1098.

Shi, Z.H., N.F. Fang, F.Z. Wu, L. Wang, B.J. Yue, and G.L. Wu. 2012. Soil erosion processes and sediment sorting associated with transport mechanisms on steep slopes. J. Hydrol. 454–455:123–130. doi:10.1016/j.jhydrol.2012.06.004

Siepel, A.C., T.S. Steenhuis, C.W. Rose, J.Y. Parlange, and G.F. McIsaac. 2002. A simplified hillslope erosion model with vegetation elements for practical applications. J. Hydrol. 258:111–121. doi:10.1016/S0022-1694(01)00569-8

Slattery, M.C., and T.P. Burt. 1997. Particle size characteristics of suspended sediment in hillslope runoff and stream flow. Earth Surf. Processes Landforms 22:705–719. doi:10.1002/(SICI)1096-9837(199708)22:8<705::AID-ESP739>3.0.CO;2-6

Smets, T., J. Poesen, and A. Knapen. 2008. Spatial scale effects on the effectiveness of organic mulches in reducing soil erosion by water. Earth Sci. Rev. 89:1–12. doi:10.1016/j.earscirev.2008.04.001

Tang, K.L. 1990. Regional characteristics of soil erosion and its control approaches on Loess Plateau (in Chinese). Science Press, Beijing. p. 42–103.

Tromp-van Meerveld, H.J., J.Y. Parlange, D.A. Barry, M.F. Tromp, G.C. Sander, M.T. Walter, and M.B. Parlange. 2008. Influence of sediment settling velocity on mechanistic soil erosion modeling. Water Resour. Res. 44:W06401. doi:10.1029/2007WR006361

Valentin, C., and L. Bresson. 1992. Morphology, genesis and classification of surface crusts in loamy and sandy soils. Geoderma 55:225–245. doi:10.1016/0016-7061(92)90085-L

Wan, Y., and S.A. El-Swaify. 1998. Characterizing interrill sediment size by partitioning splash and wash processes. Soil Sci. Soc. Am. J. 62:430–437. doi:10.2136/sssaj1998.03615995006200020020x

Warrington, D.N., A.I. Mamedov, A.K. Bhardwaj, and G.J. Levy. 2009. Primary particle size distribution of eroded material affected by degree of aggregate slaking and seal development. Eur. J. Soil Sci. 60:84–93. doi:10.1111/j.1365-2389.2008.01090.x

Wu, F.Z., Z.H. Shi, and N.F. Fang. 2012. Temporal variations of clay content in eroded sediment under different rainfall condition (in Chinese). Chinese J. Environ. Sci. 33:2497–2502.

Young, R.A. 1980. Characteristics of eroded sediment. Trans. ASAE 23:1139–1142.

Young, R.A., and C.A. Onstad. 1978. Characterization of rill and interrill eroded soil. Trans. ASAE 21:1126–1130.

Zhang, G.H., Y.M. Liu, Y.F. Han, and X.C. Zhang. 2009. Sediment transport and soil detachment on steep slopes: I. Transport capacity estimation. Soil Sci. Soc. Am. J. 73:1291–1297. doi:10.2136/sssaj2008.0145

Zhang, H.X. 1983. The characteristics of rainstorm and its distribution in the Loess Plateau (in Chinese). Acta Geogr. Sin. 38:416–425.

Zuazo, V.H.D., and C.R.R. Plequezuelo. 2008. Soil-erosion and runoff prevention by plants covers. A review. Agron. Sustainable Dev. 28:65–86. doi:10.1051/agro:2007062